HHS Public Access

Author manuscript

Cancer Res. Author manuscript; available in PMC 2018 June 29.

Published in final edited form as:

Cancer Res. 2017 April 01; 77(7): 1637–1648. doi:10.1158/0008-5472.CAN-15-3084.

YAP/TAZ-mediated upregulation of GAB2 leads to increased sensitivity to growth factor-induced activation of the PI3K pathway

Chao Wang[1,2,*,@], **Chao Gu**[1,2,@], **Kang Jin Jeong**[2], **Dong Zhang**[2], **Wei Guo**[2], **Yiling Lu**[2], **Zhenlin Ju**[3], **Nattapon Panupinthu**[2,4], **Ji Yeon Yang**[3], **Mihai (Mike) Gagea**[5], **Patrick Kwok Shing Ng**[2], **Fan Zhang**[2], and **Gordon B. Mills**[2]

[1]Department of Obstetrics and Gynecology, Obstetrics and Gynecology Hospital, Fudan University, Shanghai, 200011, China [2]Department of Systems Biology, University of Texas MD Anderson Cancer Center, Houston, TX 77030, USA [3]Department of Bioinformatics and Computational Biology, University of Texas MD Anderson Cancer Center, Houston, TX 77030, USA [4]Department of Physiology, Faculty of Science, Mahidol University, Bangkok, 10400, Thailand [5]Department of Veterinary Medicine & Surgery, University of Texas MD Anderson Cancer Center, Houston, TX 77030, USA

Abstract

The transcription regulators YAP and TAZ function as effectors of the HIPPO signaling cascade, critical for organismal development, cell growth, and cellular reprogramming, and YAP/TAZ is commonly misregulated in human cancers. The precise mechanism by which aberrant YAP/TAZ promotes tumor growth remains unclear. The HIPPO tumor suppressor pathway phosphorylates YAP and TAZ resulting in cytosolic sequestration with subsequent degradation. Here we report that the phosphatidylinositol 3′ kinase (PI3K)/AKT pathway, which is critically involved in the pathophysiology of endometrial cancer (EC), interacts with the HIPPO pathway at multiple levels. Strikingly, coordinate knockdown of YAP and TAZ, mimicking activation of the HIPPO pathway, markedly decreased both constitutive and growth factor induced PI3K pathway activation by decreasing levels of the GAB2 linker molecule in EC lines. Furthermore, targeting YAP/TAZ decreased EC tumor growth *in vivo*. In addition, YAP and TAZ total and phosphoprotein levels correlated with clinical characteristics and outcomes in EC. Thus, YAP and TAZ, which are inhibited by the HIPPO tumor suppressor pathway, modify PI3K/AKT pathway signaling in EC. The crosstalk between these key pathways identifies potential new biomarkers and therapeutic targets in EC.

[*]Corresponding Author: Chao Wang, Ob& Gyn Hospital of Fudan University, 419 Fangxie Rd, Shanghai, China wang1980-55@163.com.
[@]Equal contributions from both authors

Competing financial interests

The authors declare no competing financial interests.

Keywords

PI3K pathway; YAP; TAZ; HIPPO; GAB2

Introduction

Phosphatidylinositol 3-kinase (PI3K)/AKT pathway is aberrant in more than 90% of EC (1–4). Multiple pathway members are often coordinately mutated in EC, whereas pathway mutations are mutually exclusive in most other cancer lineages. Thus EC represents a primarily PI3K-driven disease, which has led to multiple clinical trials targeting different PI3K pathway nodes.

The HIPPO pathway is a major contributor to cancer pathophysiology. Mst1/2-Lats1/2-YAP/TAZ-TEAD constitute core mammalian HIPPO pathway components. The Yes-associated protein (YAP) and its homolog, TAZ (aka WWTR1), are key downstream effectors in the HIPPO signaling cascade(5–7). YAP and TAZ are phosphorylated by Lats1/2 resulting in cytosolic sequestration and subsequent proteosomal degradation. In the absence of HIPPO activation, YAP and TAZ translocate to the nucleus where they act as transcriptional co-activators of the TEAD program increasing production of CTGF, amphiregulin and other key regulators. Thus YAP and TAZ function as oncogenes in many cancers, with nuclear localization of YAP/TAZ correlating with poor prognosis(8). However YAP also has been implicated as a tumor suppressor under particular circumstances(9). The tumor suppressor effects may be independent of its transcriptional co-activator function with YAP acting as a cytosolic scaffolding protein (10–14). Thus YAP/TAZ likely exert context dependent effects on tumor pathophysiology. Components of the HIPPO tumor suppressor pathway are mutated in 30% of ECs and, strikingly, in 54% of ECs with microsatellite instability(1). Despite the frequency of aberrations of the HIPPO pathway, its role in EC has not been extensively explored.

HIPPO and PI3K pathways interact at multiple levels(15–19). Growth factors, including LPA, EGF and serum that activate PI3K inhibit Lats1/2 resulting in decreased YAP and TAZ phosphorylation leading to nuclear translocation and TEAD transcriptional activation(15, 18, 20). Multiple mechanisms and mediators have been proposed to contribute to cross talk between the PI3K and HIPPO pathway, and depending on the context, the PI3K pathway can both positively and negatively regulate components of the HIPPO pathway (17, 20, 21). Although YAP and TAZ have been proposed to alter PI3K/AKT signaling, the underlying mechanisms have not been delineated fully.

In this study, we investigated the mechanisms by which YAP and TAZ regulate PI3K/AKT pathway activity thus contributing to EC pathophysiology. We show GRB2-associated binding protein 2 (GAB2), which acts as a scaffold linking growth factor receptors to the PI3K and MAPK pathways, to be a key target of the HIPPO pathway. We further demonstrate that Verteporfin, an effective inhibitor of YAP/TAZ, inhibits malignant behaviors of EC cells *in vitro* and *in vivo*. Together, these studies demonstrate a previously unidentified regulatory loop whereby the HIPPO tumor suppressor pathway limits growth factor receptor signaling through the PI3K pathway with YAP and TAZ acting as redundant

regulators of the PI3K/AKT pathway. The interactions between HIPPO, YAP/TAZ and the PI3K/AKT pathway may be therapeutically targetable providing new approaches to treating EC and potentially other diseases in which the HIPPO pathway is aberrant.

Materials and Methods

Reagents and materials

Antibodies to YAP, TAZ, pAKTT308, pAKTS473, AKT, pP70S6KT389, P70S6K, pERK, Grb2, CTGF, pIGF1R, IGF1R, pGABT452, E-cadherin and β-catenin were from Cell Signaling Technology; pIRS1 and IRS1 from EMD Millipore; Erk2 from Santa Cruz Biotechnology and H3K9Me3 from Abcam.

IGF1 was from Upstate Biotechnology, EGF from Sigma and insulin from Gibco-BRL, and LPA (1-oleoyl-2-hydroxy-sn -glycero-3-phosphate) from Sigma or Avanti. Before use, LPA was solubilized in phosphate-buffered saline containing 1% fatty acid-free bovine serum albumin (Roche Molecular Biochemicals).

ON-TARGETplus SMARTpool siRNA libraries, ON-TARGETplus siRNA and siGENOME RISC-Free Control siRNA (D-001220-01) were from Dharmacon. YAP and TAZ plasmids were from Ju-Seog Lee (MD Anderson Cancer Center (MDACC)). X-tremeGENE HP DNA Transfection Reagent was from Roche Diagnostics.

TCGA data

Clinical data and reverse-phase protein array (RPPA) EC patient data were from the TCGA Data portal (http://tcga-data.nci.nih.gov/tcga/findArchives.htm).

Cell culture, transient transfection and assays

KLE, EFE184, HEC-1A, NOU-1 and SKUT-2 were from the MDACC Characterized Cell Line Core Facility and propagated as monolayer cultures with, respectively, DMEM F12, RPMI1640, McCoy's 5a medium and DMEM, supplemented with 5% heat-inactivated fetal bovine serum (FBS), except 10% FBS for NOU-1 at 37 °C in a humidified incubator containing 5% CO_2. All cell lines are validated by STR in the Core before distribution. All lines were retested for STRs and mycoplasma every 6 months. SKUT-2, HEC-1A and NOU-1 harbor activating PIK3CA mutations. None of the lines have mutations in PTEN or AKT. Of the lines assessed, only SKUT-2 reliably formed orthotopic tumors in immunodeficient mice and was thus used for in vivo studies.

RPPA

RPPA was performed in the MDACC CCSG core as described at http://www.mdanderson.org/education-and-research/resources-for-professionals/scientific-resources/core-facilities-and-services/functional-proteomics-rppa-core/index.html.

RNA-seq

RNA-seq analysis was performed on a Solid sequinator and analyzed by Nexus expression software.

Verteporfin treatment of mice

Female athymic nude mice from National Cancer Institute-Frederick Cancer Research and Development Center were housed in specific pathogen-free conditions. All studies were approved by the MDACC Institutional Animal Care and Use Committee. Mice were anesthetized with 200 μl nembutal i.p. and a 1 cm incision made in the left lower flank to expose the left uterine horn. 100 μl SKUT-2 single-cell suspension ($4x10^6$ cells) was injected into the uterine horn lumen and incision closed with staples. Mice were divided into 2 random groups by odd (treatment group (n=15)) and even number (placebo group (n=14)). Two weeks later Verteporfin in PEG400 micelles was administered intraperitoneally every 2 days at 45 mg/kg for 2 weeks. 100 mg Verteporfin dissolved in 1 ml DMSO was slowly added, with stirring. A 160 μl aliquot was added to 1.44 ml PEG400 and PBS (ratio of 2:1). Mice in control group were treated with DMSO-PEG400-PBS vehicle. Animals were euthanized after 16 days of Verteporfin treatment. Tumor volume was calculated according to the equation (length x $width^2$)/2. A portion of the tumor was returned to cell culture with tissue also fixed in formalin for histologic analysis.

Statistical analysis

In all figures, ****P<0.0001, ***P<0.001, **P<0.01, *P<0.5, ns non-significant. Statistical significance was by two way ANOVA and Sidak's multiple comparisons test unless noted otherwise. The statistical approach and number of replicates for each study is indicated in each figure legend. The robustness and generalizability of the results are supported by repeating the studies across multiple relevant cell lines.

Results

siYAP and siTAZ inhibit PI3K/AKT pathway activation

We knocked down YAP and TAZ alone and together and performed reverse phase protein array (RPPA) assessing 221 proteins including 34 phosphorylated proteins involved in multiple signaling pathways. While individual siRNA to YAP and TAZ decreased levels of a similar set of phospho and total proteins, combined knockdown of YAP and TAZ (siYAP/TAZ) had more marked effects consistent with a degree of redundancy between YAP and TAZ signaling (Fig 1a). The effect of YAP and TAZ knockdown on key proteins was confirmed by western blotting (Fig 1b). Similar effects were also seen in HEC-1A cells (Supplementary Fig 1e).

Based on Ingenuity pathway analysis (IPA) of canonical pathways, PI3K/AKT signaling was identified as one of the top 5 pathways altered by siYAP/TAZ. Endometrial Cancer Signaling ranked No. 26 out of 331 canonical pathways. Molecular and cellular functions affected by YAP and TAZ down regulation included cell death and survival, cellular development, cellular growth and proliferation, cell cycle, and cell morphology, all of which are influenced by PI3K/AKT signaling. Strikingly, the majority of molecules in the PI3K/AKT signaling pathway assessed by RPPA were perturbed by siYAP/TAZ in EFE184 (Supplementary Fig 1a) and KLE (Supplementary Fig 1b). Although siYAP/TAZ altered "the endometrial cancer signaling pathway" in the two cell lines (Supplementary Fig 1c for EFE184, Fig 1d for KLE), many proteins that comprise "the endometrial cancer signaling

pathway" in IPA analysis overlap with the PI3K/AKT signaling pathway. However, additional effects were noted on β-catenin and RAS signaling pathways that would be explained solely by perturbation of PI3K/AKT pathway. When the most significantly down-regulated molecules in the RPPA analysis were assessed, pYAP1, GAB2, pRPS6, pRPS6KB1, pEIF4EBP1 were decreased in both KLE and EFE184 whereas HIF1A, CAV1, BCL2, COPS5, pCHEK1, pRB1, MYC, CCNB1, NDRG1, and GSK3B were altered in one of the two lines. Based on the preponderance of effects on PI3K/AKT signaling, particularly when both cell lines were considered, we focused on the effects of siYAP/TAZ on PI3K/AKT signaling. KLE and EFE184 were chosen for this analysis as they do not have mutations in the canonical pathway members of the PI3K/AKT pathway including PTEN, PIK3CA and AKT, which could complicate analysis of effects on signaling. However, key effects were confirmed in SKUT-2, HEC-1A and NOU-1 that have aberrations in the PI3K pathway.

GAB2 is markedly altered by siYAP and TAZ

Meanwhile, we performed RNA sequencing (RNAseq) to investigate effects of siYAP and siTAZ on KLE and EFE184. Since we focused on effects of YAP and TAZ on PI3K/AKT signaling, we searched all probes related to "phosphatidylinositol" using Nexus expression software ($p<0.01$, comparing siControl with siYAP/TAZ). This yielded adequate signal for 179 mRNAs for EFE184 and 67 mRNA for KLE with all signals in KLE being represented in RNASeq data from EFE184. Among these mRNA, 54% (36/67) were decreased in KLE, 82% (55/67) were decreased in EFE184. 49% (33/67) were decreased in both KLE and EFE184 with siYAP/TAZ. Among these down-regulated genes, GAB2, EFNA3 and GFRA1 were markedly altered in both cell lines (Fig 2, Supplementary Fig 2). Quantitative PCR (q-PCR) validated the effect of siYAP/TAZ on GAB2 mRNA levels (Supplementary Fig 2b). Since GAB2 was decreased in both RPPA and RNASeq analysis and acts as an adapter transmitting signals from multiple activated growth factor receptors to the PI3K/AKT pathway(22, 23), GAB2 represented a likely candidate to mediate effects of YAP/TAZ on PI3K/AKT signaling. In contrast, EFNA3 and GFRA1 have not been implicated in PI3K/AKT signaling.

GAB2 is required for the effect of siYAP/TAZ on PI3K/AKT signaling

Western blots demonstrated that YAP/TAZ knockdown decreased GAB2 levels and furthermore that overexpression of YAP and TAZ increased GAB2 levels (Fig 3a, Supplementary Fig 3c). A related linker molecule, GRB2, was not substantially altered by siYAP/TAZ. CTGF, a key downstream target of YAP/TAZ(24), was used to indicate the degree of functional knockdown of YAP and TAZ. Note that in KLE, concurrent knockdown of YAP and TAZ is required to markedly decrease CTGF levels consistent with the contention that YAP and TAZ can act as redundant co-transcriptional activators of TEAD in EC cells. In EFE184, siTAZ markedly decreased CTGF, however, siYAP/TAZ was required for abrogation of CTGF expression. In EC cells, GAB2 is a key regulator of PI3K/AKT signaling as indicated by decreased pAKT T308 upon knockdown of GAB2 in KLE cells and increased pAKT S473 upon overexpression of GAB2 in HEC-1A cells (Fig 3b).

Concurrent knockdown of YAP/TAZ, but not of YAP or TAZ alone, inhibited cell proliferation even under stimulation with growth factors, including IGF1, insulin, EGF, and LPA (Fig 3c, Supplementary Fig 3a). However, the effect of coordinate knockdown of YAP and TAZ on LPA induced proliferation was less than on the other growth factors.

siYAP/TAZ almost completely blocked increases in AKT phosphorylation induced by IGF and partially inhibited EGF induced increases in KLE (Fig 3e–f) as well as decreased magnitude and duration of EGF induced increases in KLE, EFE184 and SKUT-2 (Supplementary Fig 3c). Similar effects were seen in HEC-1A demonstrating generalizability and further that the effects are present in EC cells harboring PIK3CA mutations (Fig 3e–f). In contrast, siYAP/TAZ did not inhibit increases in pERK induced by EGF. Of note, we observed that siYAP/TAZ increased pIGF1R levels, which might be due to a feedback loop activated by inhibition of PI3K/AKT signaling(25). Thus, YAP/TAZ knock down has more marked effects on PI3K/AKT signaling compared to MAPK signaling.

Strikingly, down-regulation of GAB2 inhibited cell proliferation similar to knock down of YAP and TAZ in the presence and absence of growth factors (Fig 3d). Moreover, enforced expression of GAB2 substantially reversed the inhibition of cell growth induced by siYAP/TAZ in the presence of either insulin or IGF1 (Fig 3g), consistent with GAB2 being the key mediator linking YAP and TAZ to insulin and IGF1 PI3K pathway activation. Overexpression of GAB2 did not reverse the effects of siYAP/TAZ on cell growth in the absence of exogenous growth factors (Supplementary Fig 3b) consistent with the more limited effects of siYAP/TAZ on basal cell growth as well as LPA induced cell growth.

To determine whether GAB2 is required for YAP/TAZ knockdown to decrease PI3K/AKT signaling, we determined the effect of coordinate knock down of YAP and TAZ in wild type and GAB2$^{-/-}$ murine embryo fibroblasts (MEF) (Fig 3h). As in EC lines, siYAP/TAZ decreased basal pAKT levels and IGF increased pAKTin GAB2 wild type MEF. As expected, basal pAKT levels were much lower in GAB2$^{-/-}$ MEF than in wild type MEF and while IGF increased pAKT levels in GAB2$^{-/-}$ MEF, pAKT levels remained lower than those in wild type MEFs. Critically, siYAP/TAZ did not substantially alter basal or IGF induced increases in pAKT in GAB2$^{-/-}$ MEF. Thus GAB2 is required for regulation of the PI3K pathway by YAP/TAZ.

Correlation of YAP/TAZ/GAB2 with clinical characteristics of EC patients

To investigate correlations of YAP/TAZ/GAB2 with clinical characteristics of EC patients, we analyzed protein levels of YAP, YAP phosphorylated at serine127 (pYAPS127; an inactive form of YAP), TAZ (phospho-TAZ antibodies were not included because they have not been validated for RPPA) and GAB2 in The Cancer Genome Atlas (TCGA) data (376 EC samples) which was generated in our laboratory. YAP total protein expression did not differ between early- and late-stage or between low- and high-grade disease. pYAPS127 (inactive YAP) was lower in both high-grade and late-stage disease(Fig 4a). In contrast, TAZ was elevated in high grade but not late stage disease (Fig 4b). GAB2 levels were elevated in high grade and late stage (Fig 4c). Of the potential biomarkers, pYAPS127 was associated with a markedly improved survival (Fig 4d). The association of pYAPS127 with patient survival was retained on multivariate analysis (Table 1–4 in supplementary data).

Effects of YAP/TAZ on biological behavior of EC cells

We explored effects of YAP/TAZ on biological behaviors of EC cells. We found that siYAP/TAZ inhibited cell proliferation more effectively than knockdown of either YAP or TAZ alone (Fig 5a–b, supplementary Fig 5a–b). Western blotting confirmed knockdown of YAP and TAZ as well as the expected decrease in GAB2 (supplementary Fig 5d). Overexpression of TAZ was sufficient to increase cell proliferation, whereas overexpression of YAP had more moderate effects (Supplementary Fig 5e).

We subsequently assessed effects of siYAP/TAZ on cell death and survival in 3D cultures (Fig 5c, Supplementary Fig 5c). siYAP/TAZ induced a more marked decrease in colony size and number than either siRNA alone. For KLE, the decrease in cell density was associated with increased cell death, whereas in EFE184, inhibition of cell cycle progression was more marked than cell death (Fig 5j). However, even in EFE184, cell death was induced by knockdown of YAP and TAZ (red arrow, Fig 5c).

Because we observed that siYAP/TAZ caused cells to become large and flat (Supplementary Fig 5f), characteristics associated with senescence, we assessed effects of siYAP/TAZ on H3K9Me3, a marker of cell senescence(26). Compared with siControl, siYAP/TAZ markedly increased nuclear H3K9Me3, as well as induced nuclear morphologic changes (Fig 5d), consistent with knockdown of YAP/TAZ not only inducing cell death and cell cycle arrest but also cell senescence.

We also determined the effects of siYAP/TAZ on cell migration and invasion. siYAP, siTAZ and especially siYAP/TAZ decreased invasion of EFE184 in a modified Boyden chamber assay (Fig 5e, Supplementary Fig 5g). In a wound-healing assay, siYAP/TAZ inhibited migration (Fig 5f), while overexpression of YAP/TAZ increased migration (Fig 5g). Consistent with RPPA data demonstrating that knockdown of YAP and TAZ altered β-catenin levels, western blot and immunofluorescence indicated that siYAP/TAZ increased E-cadherin and decreased β-catenin expression consistent with decreased motility and invasive capacity (Fig 5h–i, Supplementary Fig 5h). Finally, we assessed effects of siYAP/TAZ on cell cycle progression. Flow cytometry demonstrated that siYAP/TAZ induced a cell cycle arrest (Fig 5j). Consistent with the effects on cell cycle progression, siYAP/TAZ inhibited expression of FOXM1 and cyclinB1, key cell cycle regulators (Fig 5k).

Verteporfin mimics effects of siYAP/TAZ on EC cells

Verteporfin (trade name Visudyne; Novartis), which is used clinically in photodynamic therapy for neovascular macular degeneration, has been proposed to inhibit physical interactions between YAP and TEAD(27). Verteporfin induced a similar concentration dependent decrease in YAP, TAZ and GAB2 levels (Fig 6a–b). Similar to siYAP/TAZ, Verteporfin inhibited cell proliferation even under stimulation of growth factors (Fig 6c–e). Overexpression of YAP or TAZ induced a dose response shift in Verteporfin responses (Fig 6f). Furthermore, Verteporfin did not further inhibit cell proliferation when YAP and TAZ were knocked down coordinately (Fig 6g). Together this data is consistent with Verteporfin decreasing YAP and TAZ levels with subsequent effects on GAB2 and thus PI3K/AKT signaling. To test this contention, we treated AKT1 and AKT2 deleted HCT116(28)

(HCT116 does not express AKT3) with Verteporfin. AKT deletion decreased the effects of Verteporfin on cell proliferation particularly at lower doses (Fig 6h). Consistent with this result, knock down of TSC2, which is downstream of AKT, markedly decreased the effect of Verteporfin on cell proliferation (Fig 6i). Furthermore Verteporfin decreased phospho-mTOR and its downstream targets, phospho-4EBP1(Fig 6j) and phospho-S6 (Fig 6k). This is consistent with the effects of Verteporfin being dependent on decreased YAP and TAZ levels with subsequent decreases in PI3K/AKT signaling. In addition similar to YAP/TAZ knockdown, Verteporfin also dramatically induced EC cell death (Fig 6l) and cell senescence (Fig 6m). Verteporfin also induced a striking decrease of β-catenin levels (Fig 6n–o). Importantly, the effects of Verteporfin on cell proliferation were apparent in four different EC cell lines, including lines with and without PIK3CA mutations (Fig 6p). However, Verteprofin did not alter proliferation of MCF10A, which are derived from normal breast tissue (normal endometrial epithelial cell lines are not available) (Fig 6p), suggesting tumor specific effects.

Verteporfin decreases EC tumor growth *in vivo*

Based on these results, we investigated the effect of Verteporfin in a SKUT-2 orthotopic EC tumor model. SKUT-2 was selected as the other cell lines did not reliably form orthotopic tumors. Verteporfin decreased tumor number and size (Fig 7a–b) in a pilot experiment and tumor size and weight in a larger confirmation study (Fig 7c). Of interest, three buffer-treated mice had extension of tumor to the peritoneal cavity with abdominal wall adhesion whereas none of the Verteprofin-treated mice had peritoneal extension.

We cultured cells from treated and untreated orthotopic tumors to determine whether *in vivo* treatment with Verteporfin altered cell characteristics. Cells from Verteporfin-treated and control mice retained sensitivity to Verteporfin in terms of proliferation (Fig 7d), colony formation (Fig 7e), and migration (Fig 7f, Supplementary Fig 7a). Thus fourteen days *in vivo* treatment with Verteporfin was insufficient to induce irreversible resistance to Verteprofin.

Discussion

Although regulation of YAP/TAZ has been extensively characterized, cross talk between YAP/TAZ and other pathways and, in particular, homeostatic regulatory loops have not been studied to the same degree. We demonstrated that YAP/TAZ regulates the PI3K/AKT pathway through the intermediacy of GAB2 in EC cells. Thus HIPPO pathway activation with subsequent inhibition of YAP/TAZ function would be expected to inhibit the PI3K/AKT pathway. The observation is generalizable with similar effects in 5 separate EC lines (EFE184, HEC-1A, KLE, NOU-1, and SKUT-2) including EC lines with and without PIK3CA mutations, which are prevalent in EC. None of the lines assessed have mutations in PTEN, which are also common in EC, thus it remains possible that PTEN mutations could bypass the effects of YAP/TAZ on the PI3K pathway. Similar, effects were also observed in MEF suggesting that the cross talk between YAP/TAZ and the PI3K pathway is generalizable across lineages. Strikingly, while knock down of either YAP or TAZ modestly inhibited PI3K/AKT activation, coordinate knockdown of both YAP and TAZ was required

for maximal inhibition consistent with functional redundancy between YAP and TAZ in EC and potentially other cell lineages. YAP has previously been suggested to activate the PI3K/AKT pathway through induction of miR-29 with subsequent suppression of PTEN levels(29). Our data suggests that YAP and TAZ also activate PI3K/AKT signaling through altering expression of GAB2. Together these two processes may allow fine-tuning of pathway activation.

We demonstrate that GAB2 is a key intermediary between YAP/TAZ and the PI3K/AKT pathway. RNAseq and RPPA data supported GAB2 as a functionally relevant target of YAP/TAZ. Artificially increasing GAB2 expression rescued the effects of siYAP/TAZ on cell signaling and cell proliferation. Furthermore, the effects of siYAP/TAZ on cell signaling were markedly attenuated in MEFs lacking GAB2.

GAB2 has been implicated as a potential oncogene in studies of breast and ovarian cancer, leukemia, and melanoma(30–33). GAB2 is located at chromosome 11q14.1, which is frequently amplified in human cancers(34) in particular breast, ovary and lung cancers (cBioportal.org). GAB2 amplification occurs in approximately 15% of ovarian cancers with a GAB2-PI3K-ZEB1 pathway being proposed as a therapeutic target(35). In addition, GAB2 contributes to an invasive and metastatic phenotype in breast cancer(36, 37). Our data (Fig 4c) indicates that GAB2 levels are associated with stage and grade in EC suggesting that the GAB2-PI3K/AKT pathway could be a therapeutic target in GAB2-driven EC.

Verteporfin is a second-generation photosensitizer approved for treatment of age-related macular degeneration(38). Recently, it has been identified as an inhibitor of TEAD–YAP association and YAP induced liver overgrowth(27). In our study, Verteporfin inhibited tumor cell proliferation, decreased cell viability, inhibited cell migration, and induced cell senescence. Importantly Verteporfin decreased the growth of EC cells in an orthotopic model.

Verteporfin has been proposed to mediate activities independent of the HIPPO pathway (39). However, our data are consistent with the concept that Verteporfin mediates its effects on EC cells through modulating YAP/TAZ activity. Verteporfin induced a coordinate concentration-dependent decrease in YAP, TAZ and GAB2. The concentration-dependence was paralleled by effects on PI3K pathway activity as well as on cellular functions. Importantly, knock down of YAP/TAZ or deletion of AKT or TSC2 ablated effects of Verteporfin on cell proliferation. Thus, at least in EC cells, Verteporfin appears to mediate its effects through YAP and TAZ knockdown.

In summary, YAP and TAZ regulate PI3K/AKT pathway activation through the intermediacy of GAB2. Together our data indicates that YAP and TAZ could be promising targets for EC treatment and that Verteporfin warrants further exploration as a therapeutic approach in EC.

Supplementary Material

Refer to Web version on PubMed Central for supplementary material.

Acknowledgments

Financial support

Shanghai Outstanding Youth Training Plan of China (XYQ2011062) to C Wang, National Natural Science Foundation of China 2012 (NSFC 81101953) to C Gu, NCI P30CA016672, U01CA168394, P50CA098258 to GB Mills.

We thank Dr. Bert Vogelstein (Johns Hopkins Kimmel Cancer Center, Baltimore) for HCT116 Akt−/− cells, Dr. Ju-Seog Lee (MDACC) for YAP and TAZ plasmids, and Dr. Jiyong Liang for discussions.

References

1. Kandoth C, Schultz N, Cherniack AD, Akbani R, Liu Y, et al. Cancer Genome Atlas Research N. Integrated genomic characterization of endometrial carcinoma. Nature. 2013; 497:67–73. [PubMed: 23636398]
2. Rudd ML, Price JC, Fogoros S, Godwin AK, Sgroi DC, Merino MJ, et al. A unique spectrum of somatic PIK3CA (p110alpha) mutations within primary endometrial carcinomas. Clinical cancer research : an official journal of the American Association for Cancer Research. 2011; 17:1331–40. [PubMed: 21266528]
3. Cheung LW, Hennessy BT, Li J, Yu S, Myers AP, Djordjevic B, et al. High frequency of PIK3R1 and PIK3R2 mutations in endometrial cancer elucidates a novel mechanism for regulation of PTEN protein stability. Cancer discovery. 2011; 1:170–85. [PubMed: 21984976]
4. Liang H, Cheung LW, Li J, Ju Z, Yu S, Stemke-Hale K, et al. Whole-exome sequencing combined with functional genomics reveals novel candidate driver cancer genes in endometrial cancer. Genome research. 2012; 22:2120–9. [PubMed: 23028188]
5. Zhao B, Wei X, Li W, Udan RS, Yang Q, Kim J, et al. Inactivation of YAP oncoprotein by the Hippo pathway is involved in cell contact inhibition and tissue growth control. Genes & development. 2007; 21:2747–61. [PubMed: 17974916]
6. Oh H, Irvine KD. Yorkie: the final destination of Hippo signaling. Trends in cell biology. 2010; 20:410–7. [PubMed: 20452772]
7. Pan D. The hippo signaling pathway in development and cancer. Developmental cell. 2010; 19:491–505. [PubMed: 20951342]
8. Zhao B, Li L, Lei Q, Guan KL. The Hippo-YAP pathway in organ size control and tumorigenesis: an updated version. Genes & development. 2010; 24:862–74. [PubMed: 20439427]
9. Yuan M, Tomlinson V, Lara R, Holliday D, Chelala C, Harada T, et al. Yes-associated protein (YAP) functions as a tumor suppressor in breast. Cell death and differentiation. 2008; 15:1752–9. [PubMed: 18617895]
10. Azzolin L, Panciera T, Soligo S, Enzo E, Bicciato S, Dupont S, et al. YAP/TAZ incorporation in the beta-catenin destruction complex orchestrates the Wnt response. Cell. 2014; 158:157–70. [PubMed: 24976009]
11. Azzolin L, Zanconato F, Bresolin S, Forcato M, Basso G, Bicciato S, et al. Role of TAZ as mediator of Wnt signaling. Cell. 2012; 151:1443–56. [PubMed: 23245942]
12. Rosenbluh J, Nijhawan D, Cox AG, Li X, Neal JT, Schafer EJ, et al. beta-Catenin-driven cancers require a YAP1 transcriptional complex for survival and tumorigenesis. Cell. 2012; 151:1457–73. [PubMed: 23245941]
13. Barry ER, Morikawa T, Butler BL, Shrestha K, de la Rosa R, Yan KS, et al. Restriction of intestinal stem cell expansion and the regenerative response by YAP. Nature. 2013; 493:106–10. [PubMed: 23178811]
14. Levy D, Adamovich Y, Reuven N, Shaul Y. The Yes-associated protein 1 stabilizes p73 by preventing Itch-mediated ubiquitination of p73. Cell death and differentiation. 2007; 14:743–51. [PubMed: 17110958]
15. Gumbiner BM, Kim NG. The Hippo-YAP signaling pathway and contact inhibition of growth. J Cell Sci. 2014; 127:709–17. [PubMed: 24532814]

16. Basu S, Totty NF, Irwin MS, Sudol M, Downward J. Akt phosphorylates the Yes-associated protein, YAP, to induce interaction with 14-3-3 and attenuation of p73-mediated apoptosis. Molecular cell. 2003; 11:11–23. [PubMed: 12535517]
17. Ye X, Deng Y, Lai ZC. Akt is negatively regulated by Hippo signaling for growth inhibition in Drosophila. Developmental biology. 2012; 369:115–23. [PubMed: 22732571]
18. Yu FX, Zhao B, Panupinthu N, Jewell JL, Lian I, Wang LH, et al. Regulation of the Hippo-YAP pathway by G-protein-coupled receptor signaling. Cell. 2012; 150:780–91. [PubMed: 22863277]
19. Huang W, Lv X, Liu C, Zha Z, Zhang H, Jiang Y, et al. The N-terminal phosphodegron targets TAZ/WWTR1 protein for SCFbeta-TrCP-dependent degradation in response to phosphatidylinositol 3-kinase inhibition. The Journal of biological chemistry. 2012; 287:26245–53. [PubMed: 22692215]
20. Fan R, Kim NG, Gumbiner BM. Regulation of Hippo pathway by mitogenic growth factors via phosphoinositide 3-kinase and phosphoinositide-dependent kinase-1. Proceedings of the National Academy of Sciences of the United States of America. 2013; 110:2569–74. [PubMed: 23359693]
21. Lin Z, Zhou P, von Gise A, Gu F, Ma Q, Chen J, et al. Pi3kcb Links Hippo-YAP and PI3K-AKT Signaling Pathways to Promote Cardiomyocyte Proliferation and Survival. Circulation research. 2014
22. Adams SJ, Aydin IT, Celebi JT. GAB2--a scaffolding protein in cancer. Molecular cancer research : MCR. 2012; 10:1265–70. [PubMed: 22871571]
23. Hunzicker-Dunn ME, Lopez-Biladeau B, Law NC, Fiedler SE, Carr DW, Maizels ET. PKA and GAB2 play central roles in the FSH signaling pathway to PI3K and AKT in ovarian granulosa cells. Proceedings of the National Academy of Sciences of the United States of America. 2012; 109:E2979–88. [PubMed: 23045700]
24. Zhao B, Ye X, Yu J, Li L, Li W, Li S, et al. TEAD mediates YAP-dependent gene induction and growth control. Genes & development. 2008; 22:1962–71. [PubMed: 18579750]
25. Chandarlapaty S, Sawai A, Scaltriti M, Rodrik-Outmezguine V, Grbovic-Huezo O, Serra V, et al. AKT inhibition relieves feedback suppression of receptor tyrosine kinase expression and activity. Cancer Cell. 2011; 19:58–71. [PubMed: 21215704]
26. Di Micco R, Sulli G, Dobreva M, Liontos M, Botrugno OA, Gargiulo G, et al. Interplay between oncogene-induced DNA damage response and heterochromatin in senescence and cancer. Nature cell biology. 2011; 13:292–302. [PubMed: 21336312]
27. Liu-Chittenden Y, Huang B, Shim JS, Chen Q, Lee SJ, Anders RA, et al. Genetic and pharmacological disruption of the TEAD-YAP complex suppresses the oncogenic activity of YAP. Genes & development. 2012; 26:1300–5. [PubMed: 22677547]
28. Ericson K, Gan C, Cheong I, Rago C, Samuels Y, Velculescu VE, et al. Genetic inactivation of AKT1, AKT2, and PDPK1 in human colorectal cancer cells clarifies their roles in tumor growth regulation. Proceedings of the National Academy of Sciences of the United States of America. 2010; 107:2598–603. [PubMed: 20133737]
29. Tumaneng K, Schlegelmilch K, Russell RC, Yimlamai D, Basnet H, Mahadevan N, et al. YAP mediates crosstalk between the Hippo and PI(3)K-TOR pathways by suppressing PTEN via miR-29. Nature cell biology. 2012; 14:1322–9. [PubMed: 23143395]
30. Brown LA, Kalloger SE, Miller MA, Shih Ie M, McKinney SE, Santos JL, et al. Amplification of 11q13 in ovarian carcinoma. Genes, chromosomes & cancer. 2008; 47:481–9. [PubMed: 18314909]
31. Bentires-Alj M, Gil SG, Chan R, Wang ZC, Wang Y, Imanaka N, et al. A role for the scaffolding adapter GAB2 in breast cancer. Nature medicine. 2006; 12:114–21.
32. Zatkova A, Schoch C, Speleman F, Poppe B, Mannhalter C, Fonatsch C, et al. GAB2 is a novel target of 11q amplification in AML/MDS. Genes, chromosomes & cancer. 2006; 45:798–807. [PubMed: 16736498]
33. Horst B, Gruvberger-Saal SK, Hopkins BD, Bordone L, Yang Y, Chernoff KA, et al. Gab2-mediated signaling promotes melanoma metastasis. The American journal of pathology. 2009; 174:1524–33. [PubMed: 19342374]
34. Schwab M. Amplification of oncogenes in human cancer cells. BioEssays : news and reviews in molecular, cellular and developmental biology. 1998; 20:473–9.

35. Wang Y, Sheng Q, Spillman MA, Behbakht K, Gu H. Gab2 regulates the migratory behaviors and E-cadherin expression via activation of the PI3K pathway in ovarian cancer cells. Oncogene. 2012; 31:2512–20. [PubMed: 21996746]

36. Daly RJ, Gu H, Parmar J, Malaney S, Lyons RJ, Kairouz R, et al. The docking protein Gab2 is overexpressed and estrogen regulated in human breast cancer. Oncogene. 2002; 21:5175–81. [PubMed: 12140767]

37. Fleuren ED, O'Toole S, Millar EK, McNeil C, Lopez-Knowles E, Boulghourjian A, et al. Overexpression of the oncogenic signal transducer Gab2 occurs early in breast cancer development. Int J Cancer. 2010; 127:1486–92. [PubMed: 20087860]

38. Henney JE. From the Food and Drug Administration. JAMA. 2000; 283:2779. [PubMed: 10896520]

39. Zhang H, Ramakrishnan SK, Triner D, Centofanti B, Maitra D, Gyorffy B, et al. Tumor-selective proteotoxicity of verteporfin inhibits colon cancer progression independently of YAP1. Sci Signal. 2015; 8:ra98. [PubMed: 26443705]

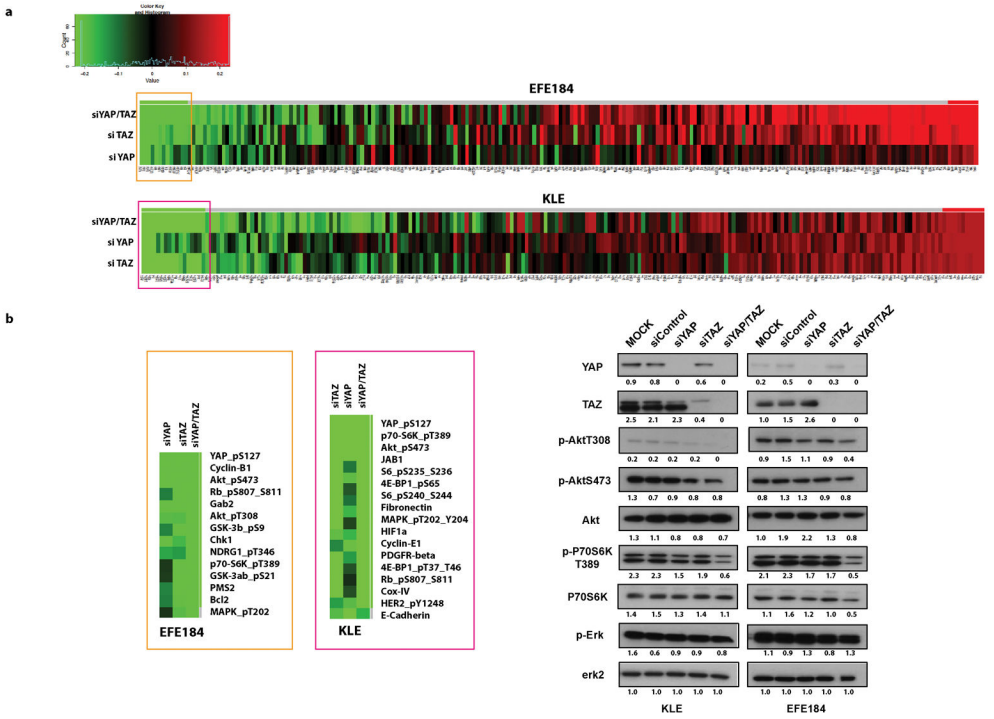

Fig 1. siYAP/TAZ inhibits PI3K/AKT pathway activation

a. EFE184 and KLE were transfected with siYAP, siTAZ and siYAP/TAZ. After 48h, cells were collected and processed for RPPA.

b. Left pictures are enlargements of frames in figure a. On the right, KLE and EFE184 were transfected with siYAP, siTAZ and siYAP/TAZ. After 48h, cell lysates were immunoblotted with indicated antibodies.

****P<0.0001, ***P<0.001, **P<0.01, *P<0.5, ns non-significant. Statistical significance was by two way ANOVA and Sidak's multiple comparisons test unless noted otherwise. The statistical approach and number of replicates for each study is indicated in each figure legend. Controls were normalized to one and the statistics represent the mean±SEM of three independent experiments with three replicates in each experiment unless noted otherwise.

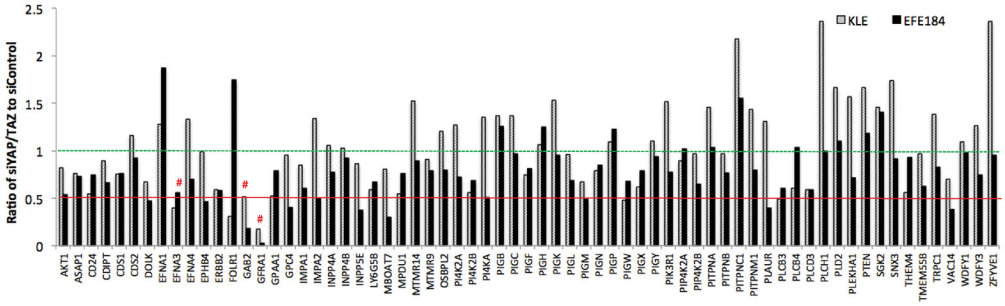

Fig 2. GAB2 mRNA is markedly altered by siYAP/TAZ

KLE and EFE184 were transfected with siYAP/TAZ and processed for RNASeq 48 hours later. Green line represents no change in gene expression. Red line indicates a 2 fold decrease in mRNA level. # represents mRNAs decreased in both lines. Results are from one of three independent experiments.

****P<0.0001, ***P<0.001, **P<0.01, *P<0.5, ns non-significant. Statistical significance was by two way ANOVA and Sidak's multiple comparisons test unless noted otherwise. The statistical approach and number of replicates for each study is indicated in each figure legend. Controls were normalized to one and the statistics represent the mean±SEM of three independent experiments with three replicates in each experiment unless noted otherwise.

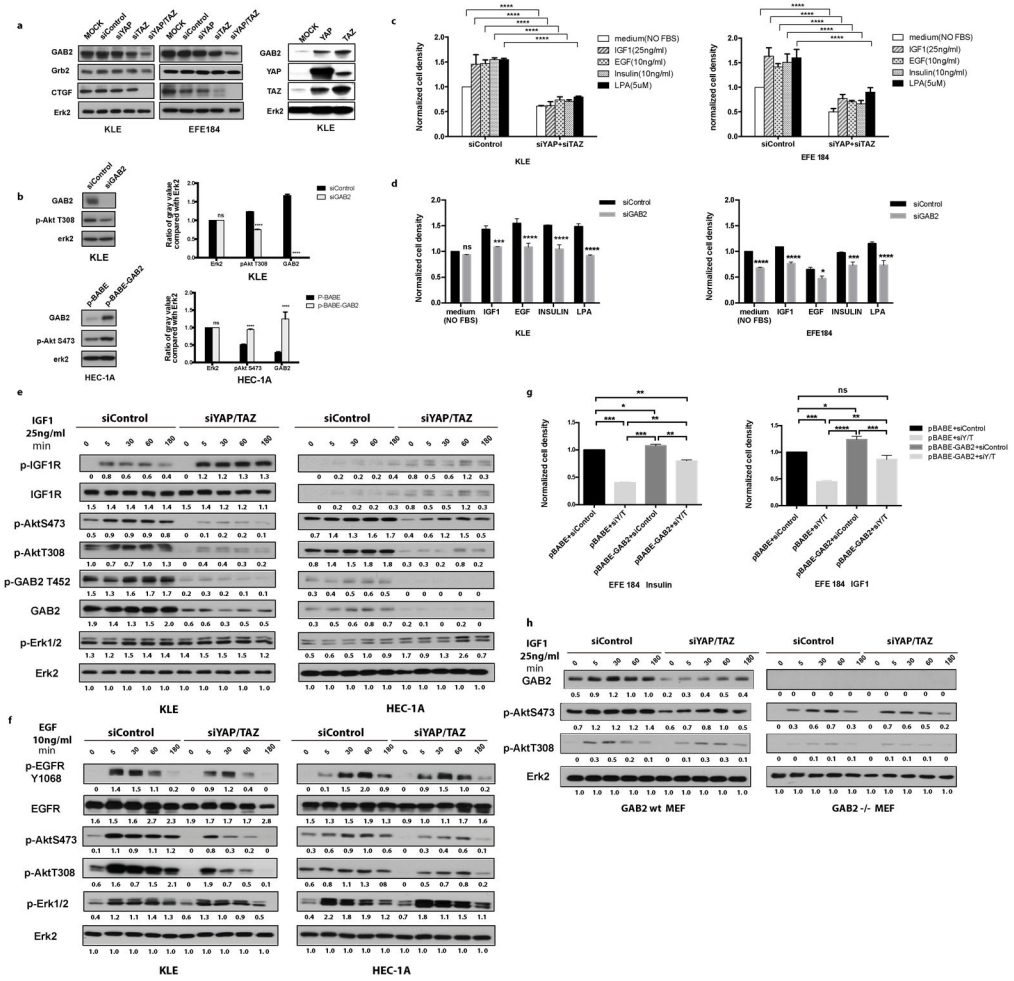

Fig 3. GAB2 mediates siYAP/TAZ effects on PI3K/AKT signaling

a. KLE and EFE184 were transfected with siYAP, siTAZ and siYAP/TAZ. KLE were transfected with YAP or TAZ plasmid. After 48h, cell lysates were immunobloted with indicated antibodies. Results are from one of three independent experiments.

b. KLE were transfected with siGAB2 and HEC-1A with GAB2 plasmid. After 48h, cell lysates were western blotted. Right side presents densitometry of western blot bands. Bars represent ratio of indicated antibodies to ERK2. Error bars are from three independent experiments.

c. KLE and EFE184 were transfected with siYAP/TAZ. After 48h, cells were starved overnight and then treated with growth factors (IGF1 25ng/ml, EGF 10ng/ml, Insulin 10ng/ml, LPA 5uM). After 72h, cells were processed for SRB staining. Error bars are from three independent experiments.

d. KLE and EFE184 were transfected with siGAB2. After 48h, cells were starved overnight and then treated with growth factors (IGF1 25ng/ml, EGF 10ng/ml, Insulin 10ng/ml, LPA 5uM). After 72h of growth factor treatment, cells were processed for SRB staining. Error bars are from three independent experiments.

e. KLE and HEC-1A cell were transfected with siYAP/TAZ. After 48h, cells were starved overnight and then treated with IGF1 25ng/ml for 5, 3, 60, and 180 min. Cells were

processed for western blotting with indicated antibodies. Numbers under bands refer to ratio of densitometry values compared to ERK2. Bands are from one of three independent experiments.

f. Cells were processed as in Fig3e except for culture with EGF 10ng/ml.

g. EFE184 were transfected with siYAP/TAZ. After 24h, pBABE-GAB2 plasmid was transfected. 48h later, cells were starved overnight and then treated with Insulin (left) or IGF1 (right). After 72h of growth factor treatment, cells were processed for SRB staining. Error bars are from three independent experiments. Statistical significance by two-tailed Student's t-test.

h. MEF GAB2 wild type cells (GAB2 wt MEF) and GAB2 knockout cells (GAB2 −/− MEF) were transfected with siYAP/TAZ. After 48h, cells were starved overnight and treated with EGF 10ng/ml for 5, 30 60, and 180 min. Cells were western blotted with indicated antibodies. Bands are from one of three independent experiments.

****P<0.0001, ***P<0.001, **P<0.01, *P<0.5, ns non-significant. Statistical significance was by two way ANOVA and Sidak's multiple comparisons test unless noted otherwise. The statistical approach and number of replicates for each study is indicated in each figure legend. Controls were normalized to one and the statistics represent the mean±SEM of three independent experiments with three replicates in each experiment unless noted otherwise.

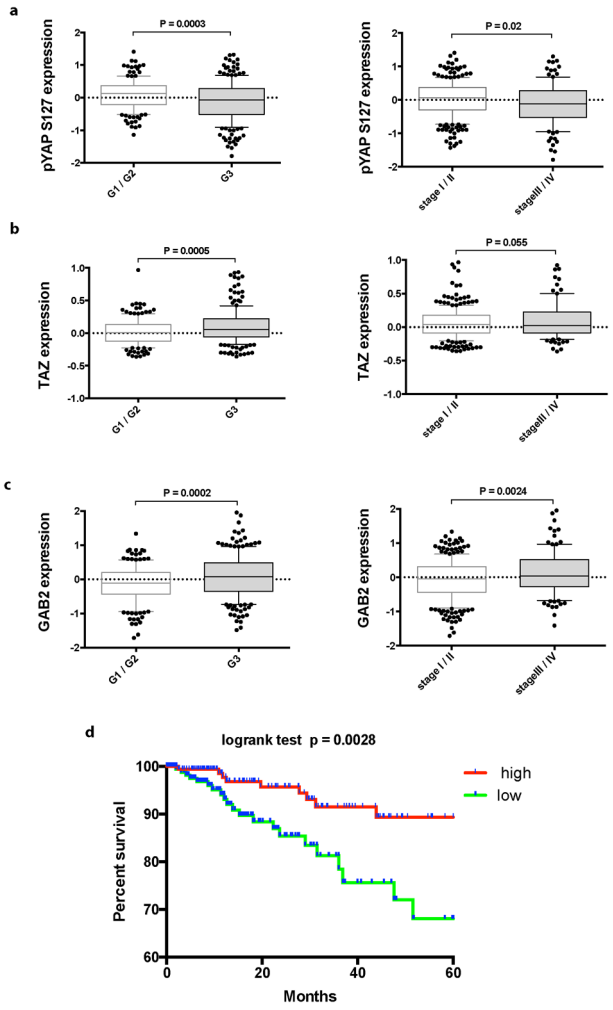

Figure 4. Correlation of YAP/TAZ/GAB2 with clinical characteristics of EC

a. pYAPS127 protein expression in 376 EC patients (TCGA). pYAPS127 protein expression was higher in Grade1/2 (G1/2) than Grade3 (G3), Unpaired t test (two tailed), p=0.0003. pYAPS127 protein expression was higher in StageI/II than StageIII/IV, Unpaired t test (two tailed), p=0.02.

b. TAZ protein expression in 376 EC patients (TCGA). TAZ protein expression was lower in G1/2 than G3, Unpaired t test (two tailed), p=0.0005.

c. GAB2 protein expression in 376 EC patients (TCGA). GAB2 protein expression was lower in G1/2 than G3, Unpaired t test (two tailed), p=0.0002. GAB2 protein expression was lower in StageI/II than StageIII/IV, Unpaired t test (two tailed), p=0.0024.

d. Correlation between pYAPS127 protein expression and 5 year patient survival (OS). Log-rank (Mantel Cox) test, P=0.0028.

****P<0.0001, ***P<0.001, **P<0.01, *P<0.5, ns non-significant. Statistical significance was by two way ANOVA and Sidak's multiple comparisons test unless noted otherwise. The statistical approach and number of replicates for each study is indicated in each figure legend. Controls were normalized to one and the statistics represent the mean±SEM of three independent experiments with three replicates in each experiment unless noted otherwise.

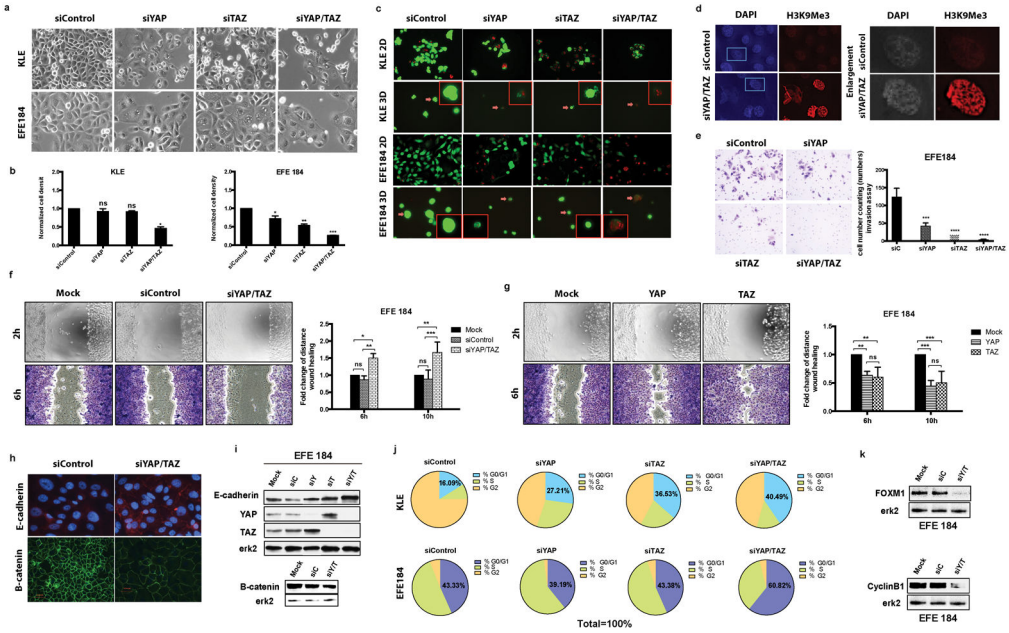

Figure 5. Effects of YAP/TAZ on biological behaviors

a. KLE and EFE184 were transfected with siYAP, siTAZ, and siYAP/TAZ. After 72h, cells were imaged. Results are from one of three independent experiments.

b. SRB assay was used to quantify cell proliferation. Error bars are from three independent experiments. Statistical significance from one-way ANOVA and Dunnett's multiple comparisons test.

c. KLE and EFE184 were transfected with siYAP, siTAZ, and siYAP/TAZ and cultured in 2D and 3D. 5 days after transfection, cells were assessed with a LIVE/DEAD kit. Red frames show enlargement of colonies with red arrows in 3D figures. Images are from one of three independent experiments.

d. EFE184 were transfected with siYAP/TAZ. After 48h, cells were stained for H3K9Me3 (red) and for DAPI (blue). Right side is enlargement of blue frame on left side. Images are from one of three independent experiments.

e. EFE184 were transfected with siYAP, siTAZ, and siYAP/TAZ. After 48h, cell invasion was assessed. Images are from one of three independent experiments. Right side is bar graph of cell numbers. Error bars are from triplicates in the experiment presented. Additional images are available in supplementary Fig 5g.

f. EFE184 were transfected with siYAP, siTAZ, and siYAP/TAZ. After 48h, wound healing was assessed. Images are from one of three independent experiments. Right side is bar graph of fold change of distance migrated. Error bars generated from triplicates in the experiment presented.

g. EFE184 were transfected with YAP and TAZ. After 48h, wound healing was assessed. Images are from one of three independent experiments. Right side is bar graph of fold change of distance migrated. Error bars generated from triplicates in the experiment presented.

h. EFE184 were transfected with siYAP, siTAZ, and siYAP/TAZ. After 48h, cells were stained with E-cadherin (red) and β cadherin (green). Images are from duplicates in one of three independent experiments. The scale bar is 100.62μM.

i. Immunoblots with indicated antibodies to determine effects of siYAP, siTAZ, and siYAP/TAZ on E-cadherin and β-cadherin levels. Bands are from one of three independent experiments.

j. KLE and EFE184 were transfected with siYAP, siTAZ, and siYAP/TAZ. After 48h, cell cycle was assessed by flow cytometry. Blue represents G0/G1 with percentages in blue. Experiments were run at 36h and 48h. The data are from a independent example of 48h.

k. Immunoblotting with indicated antibodies. Bands are from one of three independent experiments.

****P<0.0001, ***P<0.001, **P<0.01, *P<0.5, ns non-significant. Statistical significance was by two way ANOVA and Sidak's multiple comparisons test unless noted otherwise. The statistical approach and number of replicates for each study is indicated in each figure legend. Controls were normalized to one and the statistics represent the mean±SEM of three independent experiments with three replicates in each experiment unless noted otherwise.

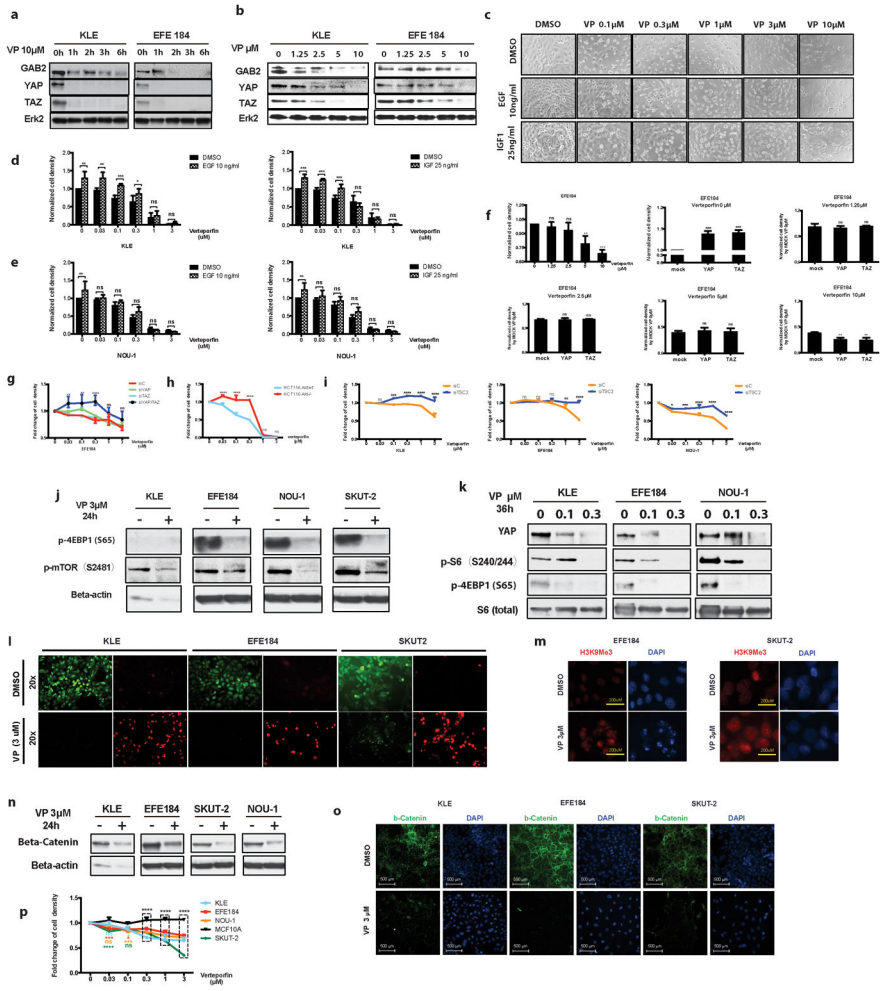

Figure 6. Verteporfin and siYAP/TAZ have similar effects

a. KLE and EFE184 were treated with 10 μM Verteporfin. After 1h, 2h, 3h, 6h, cell lysates were western blotted with indicated antibodies. Bands are from one of three independent experiments.

b. KLE and EFE184 were treated with Verteporfin (1.25 μM, 2.5 μM, 5 μM, 10 μM). After 24h, cell lysates were western blotted with indicated antibodies. Bands are from one of three independent experiments.

c. EFE184 were treated with Verteporfin (0.1 μM, 0.3 μM, 1 μM, 3 μM, 10 μM). After 24h, Verteporfin was removed and growth factors (EGF 10ng/ml, IGF1 25ng/ml) added. After 48h of growth factor treatment, cells were imaged. Images are from one of three independent experiments.

d. KLE were treated as in panel c. After 48h of growth factor treatment, cells were processed for SRB. Error bars are from three independent experiments.

e. NOU-1 were treated as in panel d.

f. EFE184 were transfected with YAP and TAZ. After 48h, cells were treated with Verteporfin (1.25 μM, 2.5 μM, 5 μM, 10 μM). After 24h of Verteporfin treatment, cells were processed for SRB. Error bars are from three independent experiments. Statistical significance by one-way ANOVA and Dunnett's multiple comparisons test.

g. EFE184 transfected with siYAP, siTAZ and siYAP/TAZ were treated with Verteporfin (0.03 μM, 0.1 μM, 0.3 μM, 1 μM, 3 μM). After 24h, cells were processed for SRB. Error bars are from three independent experiments.

h. HCT116 AKT wt and HCT116 AKT−/− were treated as in panel g. Error bars are from three independent experiments.

i. KLE, EFE184 and NOU-1 were transfected with siTSC2. The experimental and statistical methods are same as panel g. Error bars generated from three independent experiments.

j. KLE, EFE184, NOU-1 and SKUT-2 cells were treated with 3 μM Verteporfin. After 24h, cell lysates were western blotted with indicated antibodies. Bands are from one of three independent experiments.

k. KLE, EFE184 and NOU-1 were treated with Verteporfin (0.1 μM, 0.3 μM). After 36h, cell lysates were western blotted with indicated antibodies. Bands are from one of three independent experiments.

l. KLE, EFE184 and SKUT-2 cells were treated with 3 μM Verteporfin. After 24h, cells were processed for LIVE/DEAD assay. Red: dead cells, green: live cells. Images are from one of three independent experiments.

m. EFE184 and SKUT-2 cells were treated with 3 μM Verteporfin. After 24h, cells were stained for H3K9Me3 (red). Images are from one of three independent experiments. The scale bar is 200μM.

n. KLE, EFE184, NOU-1 and SKUT-2 were treated with 3 μM Verteporfin. After 24h, cell lysates were western blotted with indicated antibodies. Bands are from one of three independent experiments.

o. KLE, EFE184 and SKUT-2 were treated with 3 μM Verteporfin. After 24h, cells were stained for β-catenin (green). Images are from one of three independent experiments. The scale bar is 500μM.

p. KLE, EFE184, NOU-1, SKUT-2 and MCF10A were treated with Verteporfin (0.03 μM, 0.1 μM, 0.3 μM, 1 μM, 3 μM. After 24h, cells were processed for SRB. The error bars are from three independent experiments.

****P<0.0001, ***P<0.001, **P<0.01, *P<0.5, ns non-significant. Statistical significance was by two way ANOVA and Sidak's multiple comparisons test unless noted otherwise. The statistical approach and number of replicates for each study is indicated in each figure legend. Controls were normalized to one and the statistics represent the mean±SEM of three independent experiments with three replicates in each experiment unless noted otherwise.

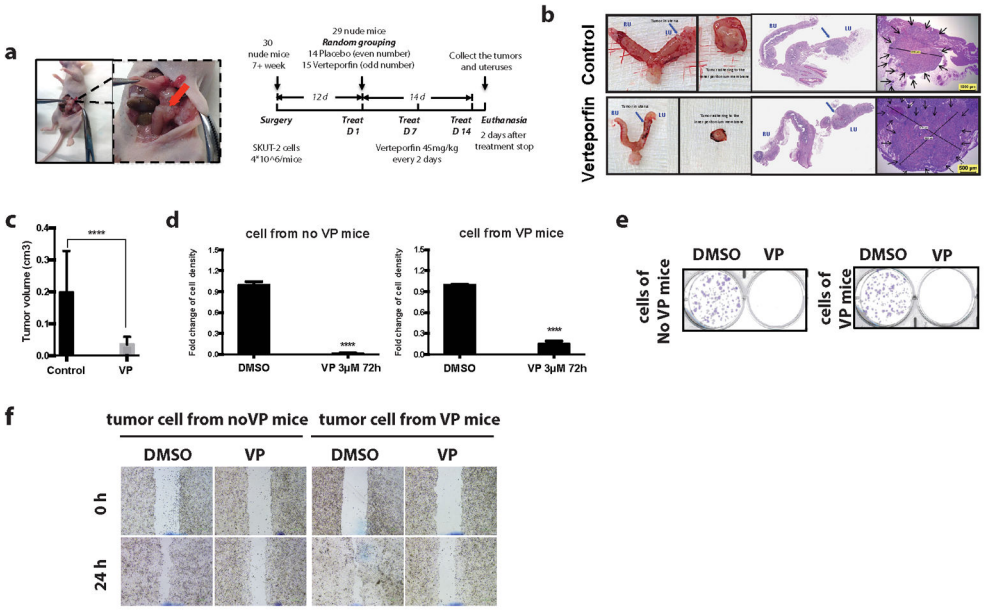

Figure 7. Effect of Verteporfin in an EC animal model

a. Pictures show tumor growing (red arrow) in left uterus horn injected with SKUT-2 ($4*10^{\wedge 6}$/mice) and adhering to inner side of peritoneum. Diagram shows experimental design.

b. Pictures show gross and microscopic images of uterus and tumors. The upper row is from control mice (placebo) in pilot experiment. The lower row is from mice treated with Verteporfin in pilot experiment. Blue arrows indicate site of injection of SKUT-2 and site of tumors growing in the uterus. Tumors were from inner peritoneum membrane, which was the site of injection through peritoneum. Slides were reviewed by a pathologist.

c. 29 mice were randomly grouped into control and test groups by odd (Verteporfin) and even numbers (controls) except for one that died after surgery. 28 mice had tumors in both uterus and peritoneum except one of the Verteporfin group where tumor was restricted to the uterus. Three control mice had large tumors connecting uterus and peritoneum. Peritoneal tumors were measured and volume calculated according to the equation (length x $width^2$)/2 since uterus tumors were too small to measure. Statistical significance by two-tailed Student t-test.

d. Cells isolated from control and Verteporfin treated mice were seeded in single cell suspension. 24h after cell seeding, cells were treated with 3 μM Verteporfin for 72h. Cells were processed for SRB. Error bars are from three independent experiments. Statistical significance by two-tailed Student t-test.

e. Cells isolated from control and Verteporfin treated mice were seeded in 6 well plates for colony formation. 24h after seeding, cells were treated with 3 μM Verteporfin for 10 days. In DMSO wells, colony numbers and size in cells of control (No Verteporfin mice) were greater and larger than those from Verteporfin treated mice. In Verteporfin treated wells, almost no cells were visible. Results from one of three independent experiments.

f. Cells from control and Verteporfin treated mice were seeded in 24 well plates. After 24h, monolayers were scratched to create an approximate 2-mm-wide wound and cells treated with 3 μM Verteporfin for 24h (see methods). Images are from a 4* objective. Images are

from one of three independent experiments. For 10* objective, please see supplementary Fig 7a.

****P<0.0001, ***P<0.001, **P<0.01, *P<0.5, ns non-significant. Statistical significance was by two way ANOVA and Sidak's multiple comparisons test unless noted otherwise. The statistical approach and number of replicates for each study is indicated in each figure legend. Controls were normalized to one and the statistics represent the mean±SEM of three independent experiments with three replicates in each experiment unless noted otherwise.